Optical properties of zinc oxide coating with an anisotropic network of nickel fibers

Guliya Nizameeva *, Viktoria Kuznetsova, Elgina Lebedeva, Irek Nizameev

Kazan National Research Technological University, Kazan 420015, Russia

* Corresponding author: guliya.riv@gmail.com

Abstract

Transparent electrodes are a special class of materials that have high electrical conductivity and transparency in the visible wavelength range. These are key elements of various devices, such as solar batteries, touch screens, etc. Previously, transparent electrodes were made of a fragile and non-ecological material – indium tin oxide (ITO). ITO has a low surface resistance of 10–25 Ohm/sq and a transmittance of more than 90%. However, the complexity of the production technology and high cost pushes researchers to find a replacement for indium tin oxide. In this paper, ZnO/NiFs films obtained by introducing an oriented network of nickel fibers (NiFs) into a thin layer of zinc oxide ZnO while maintaining its transparency in the optical range are considered an alternative to ITO. In the course of the work, a comparative analysis of the optical properties of zinc oxide films and ZnO/NiFs films with different numbers of ZnO layers was carried out. The results obtained by optical spectroscopy show that the transparency coefficient T_{550} of ZnO films, depending on the number of layers, lies in the range of 90–92%. Compared with a pure ZnO film, the value of the transparency coefficient T_{550} of the developed ZnO/NiFs system is 85%. Also, for ZnO and ZnO/NiFs films, the absorption spectra in the region of the intrinsic absorption edge were analyzed, and the band gap E_g was estimated. It was shown that the value of the band gap for zinc oxide films lies in the range of 3.23–3.26 eV. For ZnO/NiFs films, an insignificant decrease in the integral value of the band gap is observed, which lies in the range of 3.18–3.25 eV.

Key findings

● The incorporation of an oriented Ni fiber network into ZnO films preserves optical transparency.

● The transparency coefficient T_{550} of the developed ZnO/NiFs system is only 5–10% lower than that of a pure ZnO film.

● Compared to ZnO films, a slight decrease in the integral value of the band gap is observed for ZnO/NiFs, which lies in the range of 3.18–3.25 eV.

1. Introduction

Transparent electrodes are a special group of materials that have high electrical conductivity and optical transparency in the visible wavelength range. The combination of these properties makes transparent electrodes indispensable for many devices, such as touch panels, displays based on organic light-emitting diodes (OLED) and liquid crystals (LCD) [1]. Historically, the first materials for creating transparent electrodes are wide-band gap oxides [2]. Thin films of transparent conducting oxide were discovered at the beginning of the 20th century [3], as a result of which their research began, and in 1954 the first transparent electrode based on the system of indium oxide doped with tin $In_2O_3–SnO_2$ (ITO) was patented [4]. ITO has a low surface resistance of 10–25 Ohm/sq and a transmittance of more than 90%. The combination of these parameters makes ITO a sought-after transparent conductive material for opto- and photoelectronic applications [5, 6]. However, due to the growth in demand and prices for the rare material, indium, the high cost of ITO production and the impossibility of its

use in flexible devices, active research is underway into alternative materials for use as transparent electrodes [7]. Among the variety of alternative materials [8], the most interesting are conducting polymers, such as poly-3,4-ethylenedioxythiophene: polystyrene sulfonate (PEDOT:PSS) [9], carbon nanotubes (CNTs) [10, 11], metal meshes [12], graphene [13, 14], and wide-gap oxides [15]. For example, the authors of [16] used inkjet printing to obtain a highly transparent electrode based on PEDOT:PSS with a conductivity of 1213 S/cm, a surface resistance of 97 Ohm/m², and a transmittance of 86.8%. W. Jang et al. [17] studied the use of carbon nanotubes as transparent electrodes. As a result, an electrode based on CNTs with an average transmittance of 90% in the visible range was obtained. X. Feng et al. [18] studied flexible transparent electrodes based on a micro-lattice of uniformly aligned silver nanowire (AgNW) fabricated by electron printing. The resulting transparent electrode has a transmittance of 89% and a surface resistance of 5.4–91 Ohm/sq. L. Lancellotti [19] considered the use of graphene as a transparent conducting electrode. Graphene was synthesized by chemical vapour deposition with subsequent layer-by-layer deposition on substrates. It was noted that a coating of five graphene layers is characterized by a transmittance of more than 85% and a surface resistance of 100 Ohm/sq. There are also studies using a smaller amount of rare indium, which reduces the cost of transparent electrodes. T. Jantzen and his colleagues presented a material consisting of a ternary oxide system – $In_2O_3/SnO_2/ZnO$ (ZITO) as a replacement for ITO [20].

One of the key drawbacks of ITO alternative materials is the impossibility of achieving low surface resistance values while maintaining transparency since many highly conductive materials have high absorption capacity in the optical wavelength range. This problem can be solved by combining conductive wide-bandgap oxides with various dopants, which will provide an optimal combination of optical, electrophysical and mechanical properties [21].

Among transparent conductive oxides, ZnO is of particular interest in terms of its parameters [22–24]. ZnO has a wide band gap of 3.3 eV, is widespread, is non-toxic, and the methods for its production are quite diverse. This determines the potential possibility of using ZnO in both inorganic and organic optoelectronic devices, sensors and photoelectronic applications, as well as in catalysis and medicine [25]. The main methods of zinc oxide synthesis include: vapour deposition [26], molecular beam epitaxy [27], sol-gel method [28], hydrothermal method [29], spray pyrolysis [30], magnetron sputtering [31], vapour deposition with pulsed laser and thermal spraying [32], electrochemical deposition [33], annealing of zinc salts [34]. Among them, the sol-gel method is one of the most universal, due to its economic availability and the possibility of producing films with high scalability [35–37].

The method for increasing the conductivity of zinc oxide-based sol-gel films is doping with metallic or non-metallic elements (aluminium, calcium) [38–42]. L. Che et al. [43] studied transparent conducting zinc oxide films doped with fluorine (F), chlorine (Cl) and gallium (Ga). To obtain a sol-gel film, the authors used the technology of layer-by-layer deposition followed by annealing. As a result, a ZnO film containing F, Cl, and Ga atoms was obtained. The thickness of the obtained film was 380 nm. The specific resistance of the film was $1.64 \cdot 10^{-3}$ Ohm·cm, and the transparency was 90%. The authors of [44, 45] studied the possibility of improving the electrical properties of transparent conductive films based on zinc oxide by forming a composite with silver nanowires (AgNW) without reducing the transmittance. It was noted that when placing an AgNW network on a ZnO film, an electric bridge effect is observed, which provides additional electron paths, which significantly reduces the electrical resistance. S. Aghazadehchors et al. [45] proposed a two-layer coating of a silver nanowire network AgNW with zinc oxides ZnO and aluminium Al_2O_3. AgNW networks coated with ZnO demonstrated an average transmittance of 64.9% in the visible range (380–700 nm), while the application of a second layer of Al_2O_3 led to an increase in the transmittance to a value of 73.5%. D. Tigan et al. [46] presented copper nanowires CuNW as a cheap alternative to silver nanowires. However, due to the easy oxidation of CuNW even at room temperature, it is necessary to use a protective shell for them. In the work, the authors used two oxides ZnO and Al_2O_3 as protection. Chemically stable transparent conductive coatings can be obtained based on highly oriented nanowire networks of metals such as platinum and palladium [47, 48], which are not susceptible to oxidation. However, the high cost of noble metals encourages researchers to search for inexpensive but effective materials.

A good alternative to noble metals can be a network of nickel submicron wires due to its cost. Nickel has good electrical conductivity and chemical resistance. This paper presents a method for introducing a continuous and oriented network of nickel fibers into a thin layer of zinc oxide while maintaining its transparency in the optical range. Nickel and zinc oxide are available, easily synthesized and quite resistant to atmospheric influences. Many contact areas of individual particles arise when creating a layer of nanoparticles, which affects the total resistance of the material [49, 50]. To reduce this effect, it is proposed to use an oriented network of nickel fibers covered with a layer of zinc oxide. The simplicity of the production method and the low cost of the materials used will ensure that the developed material can be applied to modern devices. The synthesis method, involving chemical reduction and magnetic alignment, is relevant for industrial scalability. Synthesis in the array of small cells is assumed in the developed method since achieving magnetic field homogeneity in large areas is much more difficult than in individual small cells. This method is easily scalable.

2. Experimental

2.1. Synthesis

The sol-gel method was used to synthesize zinc oxide ZnO. 0.75 M zinc acetate dihydrate Zn $(CH_3COO)_2 \cdot 2H_2O$ in monoethanolamine (MEA) were used as starting reagents for the sol synthesis. 460 μl 2-methoxyethanol (2-ME) was used as a solvent. The synthesis was carried out with constant stirring at a temperature of 60 °C for 5 h.

The synthesis of submicron nickel fibers NiFs was carried out by the method of chemical deposition of nickel from the liquid phase. For this purpose, a 0.1 M solution of nickel chloride hexahydrate $(NiCl_2 \cdot 6H_2O)$ and a 1.5 M solution of NaOH in ethylene glycol (EG) was prepared. After that, 13 M hydrazine hydrate $(N_2H_4 \cdot H_2O)$ in EG was added to the resulting solution containing $NiCl_2 \cdot 6H_2O$ and NaOH. The finished reaction system was placed in a uniform magnetic field. The synthesis was carried out for 6 hours at a temperature of 70 °C.

2.2. Preparation of ZnO and ZnO/NiFs films

The synthesized sol was applied by centrifugation onto the surface of glass substrates with dimensions of 25×20×1 mm. To obtain ZnO films (***film 1***), each applied sol layer was annealed at a temperature of 350 °C for 20 min. The substrates were preliminarily prepared by mechanical fine cleaning and degreasing. Cleaning and degreasing were carried out using distilled water, acetone and isopropanol, which can be replaced with ethanol. The final cleaning process consisted of immersing the substrate in isopropanol and rinsing due to translational movements in the volume of liquid. After that, the surface of the glass substrate was washed with distilled water. The surface was dried with a stream of air. Particular attention was paid to the preliminary preparation since proper preparation of the surface of glass substrates is the key to obtaining high-quality coatings. The surface roughness R_a of the glass substrates prepared in this way was approximately 3.24 nm.

During the work, 5 samples were prepared with different numbers of ZnO layers on the glass surface: 1, 5, 10, 15 and 20 layers.

The ZnO/NiFs films were prepared as follows: the synthesized sol was applied to the surface of a pre-cleaned glass substrate layer by layer by centrifugation and annealed at a temperature of 350 °C for 20 min. The synthesized nickel fibers were applied to the surface of a ZnO sublayer in the form of a network. A magnetic field was used to obtain a network of fibers [51–53]. In this method, nickel fibers are introduced between zinc oxide layers. The ZnO-NiFs system resembles a sandwich structure. The layer of the oriented network of Ni fibers is located as close as possible to the top of the film, which helps improve the electrical conductivity of its surface layer as a whole. As a result, composite film based on ZnO and NiFs were obtained, which will be further designated as ZnO/NiFs (***film 2***).

2.3. Measurements

The transmission spectra of ZnO and ZnO/NiFs films were obtained on a Shimadzu UV-3600 spectrophotometer in the wavelength range λ = 350–1000 nm. The film thickness was determined from the transmission spectra using the envelope method, and the band gap was estimated.

SEM images of ZnO and ZnO/NiFs films were obtained on a Carl Zeiss EVO 50 XVP (HV = 20 kV, WD = 9 mm) scanning electron microscope. The surface morphology, particle size distribution and roughness of ZnO films were studied on a Veeco MultiMode V atomic force microscope (AFM) in intermittent contact mode.

The elemental composition of ZnO and ZnO/NiFs films was studied by X-ray fluorescence analysis (XRF) using a Thermo Scientific energy-dispersive X-ray (EDX) attachment of a Hitachi HT7700 transmission electron microscope. The accelerating voltage was 80 kV, and the accumulation time per spectrum was 300 s.

3. Results and Discussion

The first stage of this work was to obtain a pure zinc oxide film using a simple and inexpensive sol-gel method. During the AFM studies, it was established that the ZnO film has a granular structure (Figure 1).

The grain sizes are up to 90 nm. In addition, the film surface roughness, which is an important parameter determining the optical properties of transparent coatings, was determined from the AFM results. According to the results, the surface roughness R_a for the ZnO film is 5 nm. The roughness value is close to the roughness of the glass substrate (R_a = 3.24 nm). This indicates a homogeneous composition and high quality of the manufactured zinc oxide films. To confirm the elemental composition of the synthesized ZnO films, energy-dispersive X-ray analysis (point XRF) was performed. Figure 2 shows the EDX spectrum of the ZnO film. The spectrum clearly shows the lines of zinc (Lα = 1.01 keV, Kα = 8.64 keV, Kβ = 9.57 keV) and oxygen (Kα = 0.53 keV). The spectrum also contains lines corresponding to the substrate on which the studies were carried out: lines of carbon ($K\alpha_1$ = 0.28 keV) and copper ($L\alpha_1$ = 0.93 keV, $K\alpha_1$ = 8.05 keV, $K\beta_1$ = 8.90 keV).

Transparent conductive coatings are of applied interest on the surface of a glass substrate. The transmission spectra of ZnO films with different numbers of layers deposited on a glass substrate are shown in Figure 3.
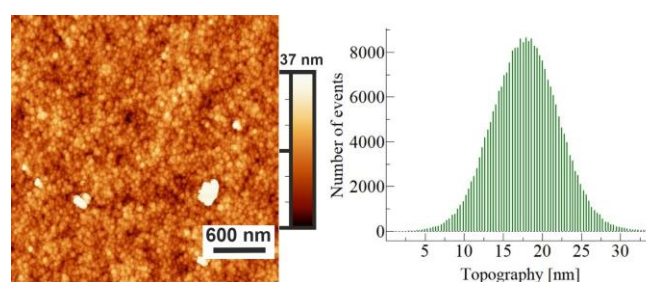

Figure 1 AFM image of ZnO film: left – topography, right – topographic histogram.
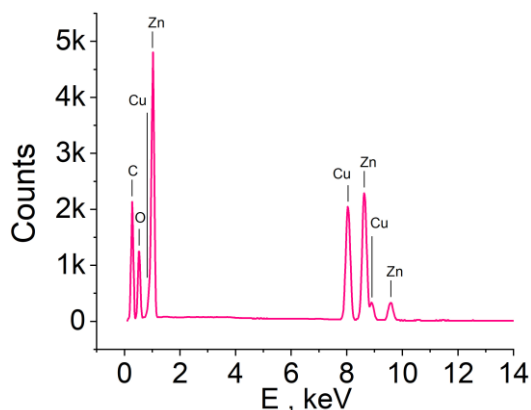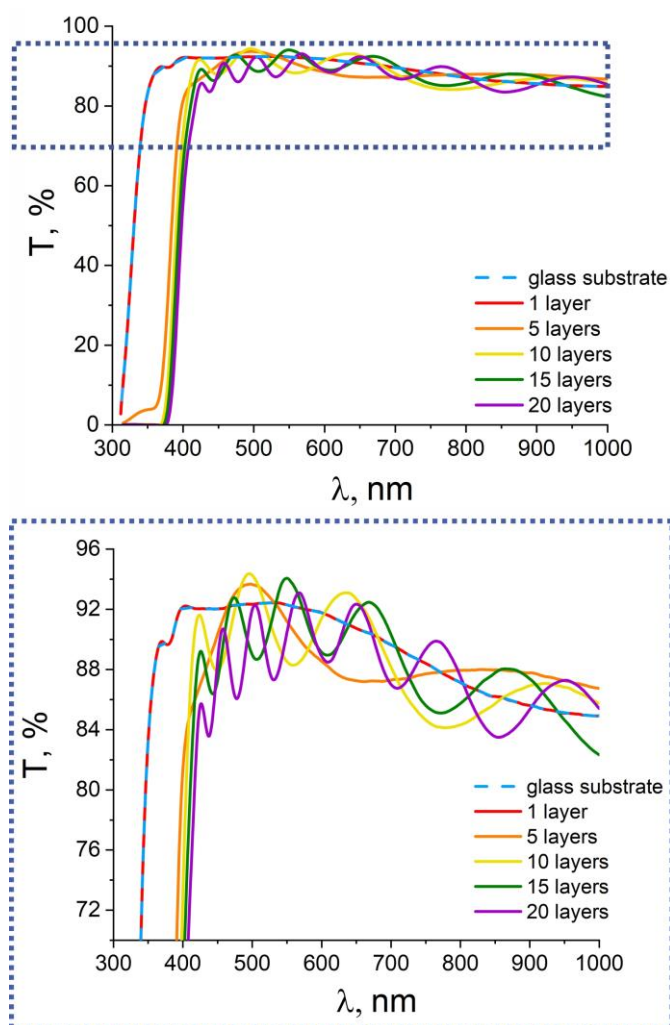
Figure 2 EDX spectrum for. *film 1*.

Figure 3 Transmission spectra of glass substrate and ZnO films with different number of layers: full range (the top image) and selected area (the bottom image).

The figure shows that the glass substrate remains transparent in the wavelength range λ = 380–720 nm. The transmittance of the glass substrate at a wavelength of 550 nm (T_{550}) is 92.3%. The transmission spectra of the ZnO films differ from the transmission spectra of the clean substrate and have a wave-like (oscillating) character. This behaviour is due to interference phenomena that occur in thin films when the film thickness is much smaller than the substrate thickness and is commensurate with the wavelength of the

radiation in question (in this case, optical radiation). The presence of interference maxima and minima in the presented transmission spectra makes it possible to determine the film thickness as well as the band gap E_g using the envelope method (the method of two envelopes $T_{max}(\lambda)$ and $T_{min}(\lambda)$) [54,55]. The envelope curves $T_{max}(\lambda)$ and $T_{min}(\lambda)$, which are the basis of the envelope method, were constructed for ZnO samples with 15 and 20 layers. For clarity, Figure 4 shows the transmission spectrum of a ZnO film (20 layers) together with the envelope curves $T_{max}(\lambda)$ and $T_{min}(\lambda)$.

After constructing the envelope curves, the spectral dependence of the refractive index n of ZnO films on the wavelength λ was determined (equation 1). This made it possible to calculate the thickness d of films with 15 and 20 ZnO layers using equation 4:

$$n = \left[N + (N^2 - n_S^2)^{\frac{1}{2}}\right]^{\frac{1}{2}},\tag{1}$$

where

$$N = 2n_S \frac{T_M - T_m}{T_M T_m} + \frac{n_s^2 + 1}{2}\tag{2}$$

and

$$n_S = \frac{1}{T_S} + \sqrt{\frac{1}{T_S^2} - 1}\tag{3}$$

where n_S is the refractive index of the substrate, T_S is the transmittance of the substrate;

$$d = \frac{A\lambda_1\lambda_2}{2(n_1\lambda_2 - n_2\lambda_1)},\tag{4}$$

where λ_1 and λ_2 are the wavelengths that correspond to adjacent extreme points on the transmission spectrum, n_1 and n_2 are the refractive indices of the films at λ_1 and λ_2, A = 1 for two adjacent extrema of the same type (max –max, min–min) and A = 0.5 for two adjacent extrema of the op-posite type (max–min, min–max).
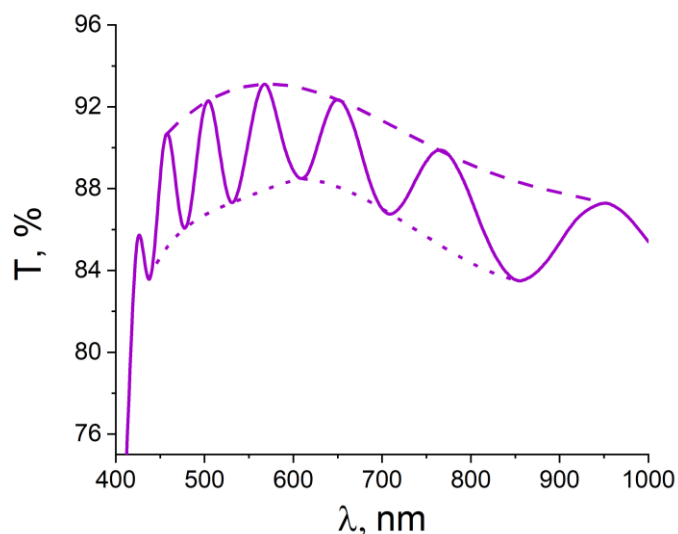

Figure 4 Transmission spectrum of ZnO film (20 layers) together with $T_{max}(\lambda)$ and $T_{min}(\lambda)$ envelopes.

The average film thickness values d are presented in Table 1. The table also shows the values of the transparency coefficient T (%) for ZnO films with different numbers of layers. As expected, with an increase in the thickness of the ZnO films, a decrease in the transparency coefficient T (%) is observed over the entire optical range.

For samples with 1, and 5 ZnO layers, the construction of $T_{max}(\lambda)$ and $T_{min}(\lambda)$ curves is not possible due to the absence and insufficient number of extrema in the considered wavelength range. Due to the impossibility of determining the thickness of a single-layer ZnO film from transmission spectra, an attempt was made to determine the film thickness by probe lithography using an atomic force microscope. The AFM image of a ZnO surface with an area of 5x5 μm and the cross-section profile along the specified line are shown in Figure 5. It was found that the thickness of one film layer is 65±10 nm. This value is in good agreement with the results of the envelope method (Table 1).

An important parameter characterizing the applicability of films as optically transparent electrodes, in addition to transparency, is the band gap E_g. From the transmission spectra of the samples (Figure 3), it is evident that the edge of the absorption band is proportional to the thickness of the ZnO films and shifts toward longer waves with its increase. Accordingly, the band gap E_g of thin zinc oxide films can be determined using the Tauc equation:

$$\alpha h v^x = h v - E_g, \tag{5}$$

where α is the absorption coefficient of the sample, h is Planck's constant, v is the frequency, x is the coefficient depending on the nature of the electronic transition. In this work, the value of x was taken to be equal to ½, since ZnO is characterized by direct allowed optical transitions.

For zinc oxide films with different numbers of layers, the dependences of $\alpha h v^{1/2}$ on the photon energy E were constructed (Figure 6).

Table 1 Thickness d and transparency coefficient T_{550} of ZnO films depending on the number of layers.

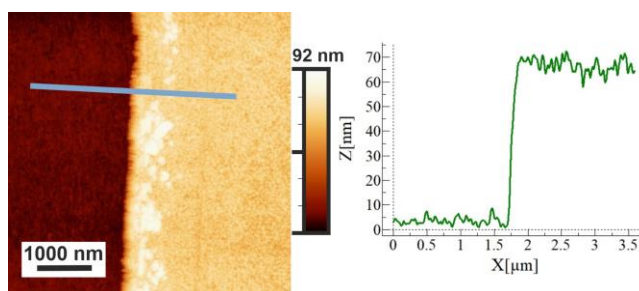| Number of layers	Thickness d, nm	1 layer thickness, nm	T_{550}, %
1	–		92.3
5	–		91.2
10	695	69.5	91.5
15	997±110	66.5	91.7
20	1309±140	65.6	90.3

Figure 5 AFM image of ZnO film: topography (left), cross-section profile along the indicated line (right).
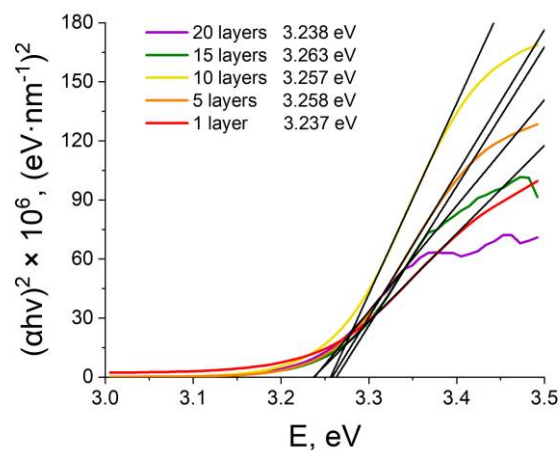

Figure 6 Dependence of $\alpha h v^{1/2}$ on E for ZnO films.

For the obtained curves, the straight section was determined and extrapolated to the point of intersection with the abscissa axis, which corresponds to the value of the band gap. According to the obtained data, the band gap for the studied ZnO films lies in the range of 3.23–3.26 eV, which is in good agreement with the literature data [56, 57].

It is known that pure zinc oxide films do not have high electrical conductivity. In order to reduce the electrical resistance of the material while maintaining transparency in the optical range, nickel fibers were introduced into ZnO films with different numbers of layers. The peculiarity of this work is that the fibers were introduced into the ZnO matrix not randomly, but in the form of an oriented network. It is assumed that the use of a system of oriented nickel fibers will reduce the percolation threshold at which a conductivity channel arises inside the ZnO film. The SEM image of the zinc oxide film on the surface of a glass substrate decorated with nickel fibers ZnO/NiFs is shown in Figure 7. The nickel fibers in the zinc oxide film are located in the form of a highly oriented network. As can be seen from the figure, the density of the fiber packing is low, and there are large gaps between the fibers, which will ensure the transparency of the film.

The elemental composition of the synthesized ZnO/NiFs film was studied by the point XRD method. Figure 8 shows the spectrum of ZnO/NiFs. The spectrum contains lines of zinc (Lα = 1.01 keV, Kα = 8.64 keV, Kβ = 9.57 keV), oxygen (Kα = 0.53 keV), and nickel lines (Kα = 7.48 keV, Kβ = 8.27 keV) are also clearly visible. The spectra also contain lines corresponding to the substrate: lines of carbon (Kα₁ = 0.28 keV) and copper (Lα₁ = 0.93 keV, Kα₁ = 8.05 keV, Kβ₁ = 8.90 keV).

Figure 9 shows the transmission spectra of ZnO/NiFs films. Table 2 shows the transmittance coefficients T of ZnO/NiFs coatings consisting of 1, 5, 10, 15, and 20 ZnO layers at a wavelength of 550 nm. According to the data presented in Table 2, the coefficient T_{550} for ZnO/NiFs composite films is in the range of 84–92%, which meets the requirements for optoelectronic elements (transparency not less than 80%).
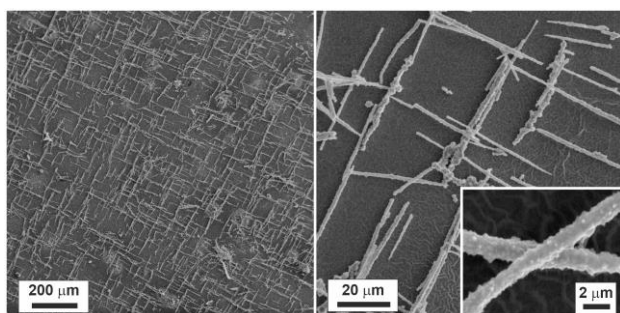
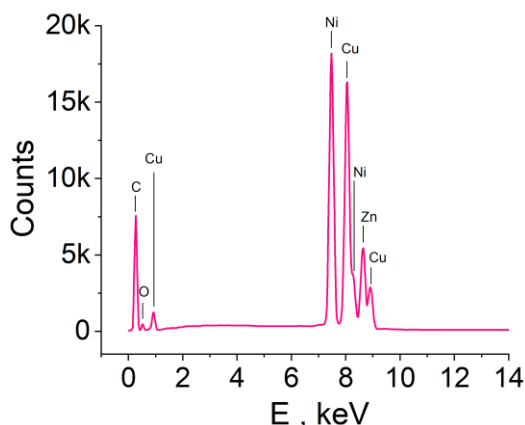**Figure 7** SEM images of ZnO/NiFs films on a glass substrate surface.
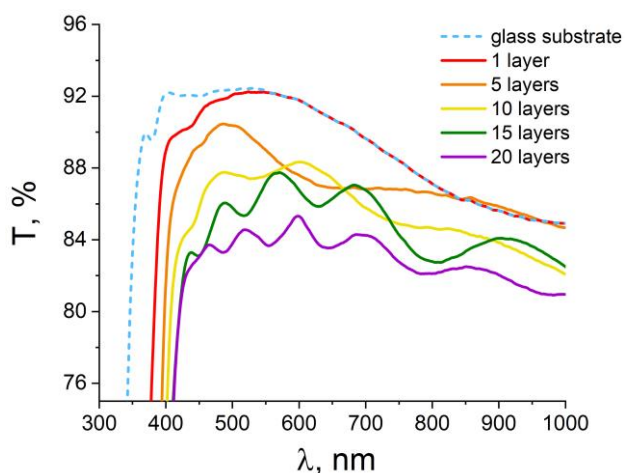

Figure 8 EDX spectrum for *film 2*.

Figure 9 Transmission spectra of ZnO/NiFs coatings on the surface of a glass substrate.

Table 2 Transparency coefficients of T_{550} ZnO/NiFs coatings.

Number of layers	Thickness d, nm	1 layer thickness, nm	T_{550}, %
1			92.3
5			89
10	833±70	83.3	88
15	1204±110	80.2	86.7
20	1646±150	82.3	84.3

The AFM image of a *film 2* surface and the cross-section profile along the specified line are shown in Figure 10. It was found that the thickness of one film layer is 80 nm. This value is in good agreement with the results of the envelope method (Table 2).

Next, the absorption spectra of ZnO/NiFs films in the region of the intrinsic absorption edge were analyzed and the band gap E_g was estimated using the Tauc method (Figure 11). Taking into account direct allowed optical transitions, the band gap for ZnO/NiFs films lies in the range of 3.18–3.25 eV.

Pure nickel is a chemically active metal and tends to form a very thin shell of its oxide on its surface. This shell protects the metal from further oxidation processes. Even though the nickel oxide shell is very thin when nickel fibers are introduced into the zinc oxide film, a Ni-NiO-ZnO transition region is formed. This leads to the formation of a heterojunction at the interface [56–58]. The positions of the valence band and conduction band edges of ZnO and NiO on the energy diagram are slightly shifted relative to each other [57]. This may lead to a slight decrease in the band gap of the system. This may probably explain the changes in E_g when introducing nickel fibers into the ZnO film.

The investigations showed that it is possible to maintain transparency of the zinc oxide layer in the optical range by introducing the continuous and oriented network of nickel fibers into the layer. Comparing the transmission spectra for pure ZnO films and modified ZnO-NiFs (Figure 3 and Figure 9), it can be seen that with an increase in the number of layers for the *film 1*, a shift in the transmission band towards longer wavelengths (420 nm) is observed. For the modified *film 2*, the left boundary of the transmission band remains in the region of 405 nm. This may be due to a slight decrease of the bang gap E_g with the preservation of good transparency in the optical range.
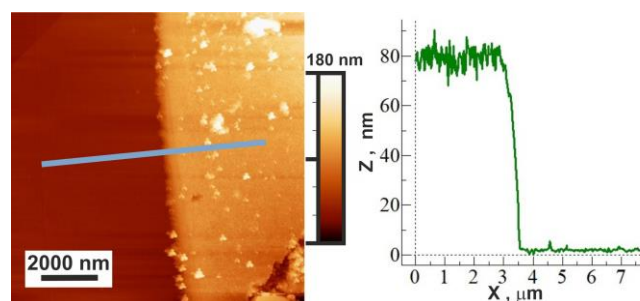

Figure 10 AFM image of ZnO/NiFs (*film 2*): topography (left), cross-section profile along the indicated line (right).
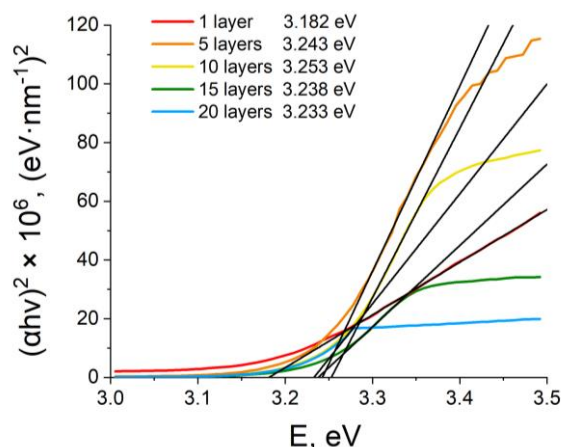

Figure 11 Dependence of αhv$^{1/2}$ on E for ZnO/NiFs films.

An essential part of the search for new materials in the field of transparent electrodes is the measurement of the conductivity. Within the framework of this work, it was planned to study the suitability of the proposed concept for the future creation of an electrically conductive coating (in terms of transparency in the optical range). Therefore, the detailed investigations of electrical conductivity were not included in this work. At the moment, we have only carried out preliminary sheet resistance measurements. It has been established that by introducing a network of nickel fibers it is possible to reduce the surface resistance (R_S) of zinc oxide by approximately 40 times while maintaining the transparency T_{550} in the range of 80–85% (Table 3). By increasing the amount of introduced nickel fibers (surface density of the network) it is possible to reduce R_S to a value of approximately 500 Ohm/sq. However, the transparency T_{550} in this case falls below 55% (Figure 12).

Table 3 compares the properties of the transparent conductive films prepared via different processes.
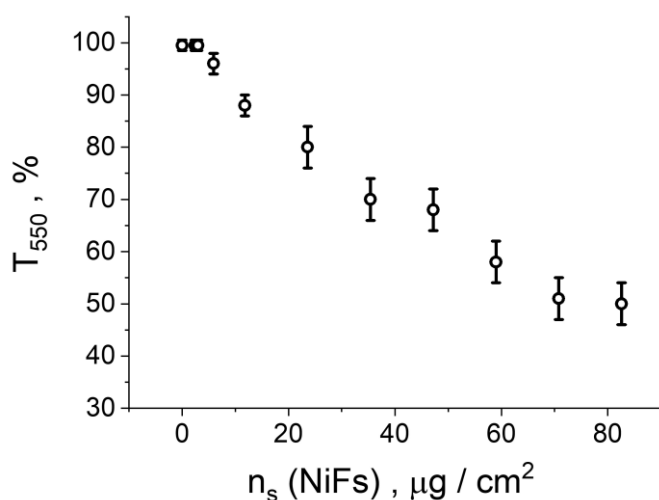

Figure 12 Transmittance at 550 nm versus the surface density of the Ni network.

4. Limitations

For a more complete and systematic analysis of the properties of the obtained material as an optically transparent conductive coating, it is necessary to carry out investigations to determine the effect of the nickel amount introduced into the zinc oxide film on the optical and electrical properties. It is also necessary to determine the optimal amount of nickel (the density of the oriented network), at which transparency is preserved and high electrical conductivity of the material is created. However, this is beyond the scope of this study, in which we primarily wanted to demonstrate that the effect of nickel nanofibers on the optical properties is insignificant.

5. Conclusions

As a result of the work performed, it was shown that the introduction of a continuous and oriented network of nickel fibers into a thin layer of zinc oxide allows retaining its transparency in the optical range. It was shown that for the developed ZnO/NiFs system, the transparency coefficient T_{550} decreased by only 5–10% compared to a pure ZnO film. For the ZnO/NiFs film, an insignificant decrease in the integral value of the band gap is observed compared to ZnO, which in this case can be characterized as an insignificant shift of the transmission spectrum towards the UV region with the preservation of good transparency in the optical range. Surface resistance studies demonstrated that by introducing a network of nickel fibers it is possible to reduce the surface resistance (R_S) of zinc oxide by approximately 40 times while maintaining the transparency T_{550} in the range of 80–85%. It was established that by increasing the amount of introduced nickel fibers (surface density of the network) it is possible to reduce R_S to a value of approximately 500 Ohm/sq. However, the transparency T_{550} in this case falls below 55%.

Table 3 Properties of the transparent conductive films prepared via different processes.

TCE film	Deposition processes	T (%) at 550 nm	Rs (Ohm/sq)	Ref.
ITO	Spin coating of the sol-gel solution	90.2	30	59
ITO	magnetron sputtering	>90	10–25	5
Graphene	CVD	85	100	19
Carbon nanotubes	CVD	90	41	60
Ag nanowires network	Electrohydrodynamic printing	99	91	18
Ag nanowires / ZnO	Spin coating of the sol-gel solution	84	40	61
Ni fibers / PEDOT:PSS	chemical deposition and magnetic alignment	75	35	52
Ni fibers / ZnO (10 µg/cm²)	chemical precipitation and magnetic alignment / spin coating of the sol-gel solution	85	10^6	this work
Ni fibers / ZnO (70 µg/cm²)	chemical precipitation and magnetic alignment / spin coating of the sol-gel solution	55	500	this work

Supplementary materials

No supplementary materials are available.

Data availability statement

The raw/processed data required to reproduce the above findings cannot be shared at this time as the data also forms part of an on-going study.

Acknowledgments

None.

Author contributions

Conceptualization: G.R.N., I.R.N.
Data curation: G.R.N., I.R.N.
Formal Analysis: G.R.N., I.R.N.
Funding acquisition: G.R.N.
Investigation: V.V.K., E.M.L., G.R.N.
Methodology: I.R.N., G.R.N, V.V.K., E.M.L.
Project administration: G.R.N.
Resources: G.R.N., I.R.N.
Software: G.R.N., I.R.N.
Supervision: G.R.N.,
Validation: G.R.N., I.R.N.
Visualization: V.V.K., G.R.N., I.R.N.
Writing – original draft: G.R.N., I.R.N.
Writing – review & editing: G.R.N., I.R.N.

Conflict of interest

The authors declare no conflict of interest.

Additional information

Author IDs:
Guliya R. Nizameeva, Scopus ID 57204606299;
Viktoria V. Kuznetsova, Scopus ID 59421978800;
Elgina M. Lebedeva, Scopus ID 58568898200;
Irek R. Nizameev, Scopus ID 35799942900;

Website:
Kazan National Research Technological University, https://www.kstu.ru/knrtu/index_en.jsp;

References

1. Wang T, Lu K, Xu Z, Lin Z, Ning H, Qiu T, Yang Z, Zheng H, Yao R, Peng J. Recent developments in flexible transparent electrode. Crystals. 2021;11(5):511. doi:10.3390/cryst11050511
2. Shi J, Zhang J, Yang L, Qu M, Qi DC, Zhang KHL. Wide bandgap oxide semiconductors: from materials physics to optoelectronic devices. Adv Mater. 2021;33(50):2006230. doi:10.1002/adma.202006230
3. Badeker K. Concerning the electricity conductibility and the thermoelectric energy of several heavy metal bonds. Ann Phys. 1907;22:749.
4. Rupprecht G. Electric and photoelectric conductivity of thin layers of indium oxide. Z Physik. 1954;139:504–17.
5. Li D, Lai WY, Zhang YZ, Huang W. Printable transparent conductive films for flexible electronics. Adv Mater. 2018;30(10):1704738. doi:10.1002/adma.201704738
6. Kim DS, Jung JY, Seo S, Kim JH. Facile fabrication of multifunctional transparent electrodes via spray deposition of indium-tin-oxide nanoparticles. Appl Surf Sci. 2023;611:155756. doi:10.1016/j.apsusc.2022.155756
7. Azani MR, Hassanpour A, Torres T. Benefits, problems, and solutions of silver nanowire transparent conductive electrodes in indium tin oxide (ITO)-free flexible solar cells. Adv Energy Mater. 2020;10(48):2002536. doi:10.1002/aenm.202002536
8. Sharma S, Shriwastava S, Kumar S, Bhatt K, Tripathi CC. Alternative transparent conducting electrode materials for flexible optoelectronic devices. Opto-Electron Rev. 2018;26(3):223–35. doi:10.1016/j.opelre.2018.06.004
9. Zhang Y, Ng SW, Lu X, Zheng Z. Solution-processed transparent electrodes for emerging thin-film solar cells. Chem Rev. 2020;120(4):2049–122. doi:10.1021/acs.chemrev.9b00483
10. Jeon I, Yoon J, Kim U, Lee C, Xiang R, Shawky A, Xi J, Byeon J, Lee HM, Choi M, Maruyama S, Matsuo Y. High-performance solution-processed double-walled carbon nanotube transparent electrode for perovskite solar cells. Adv Energy Mater. 2019;9(27):1901204. doi:10.1002/aenm.201901204
11. Mustafin IA, Akhmetov AF, Salikhov RB, Mullagaliev IA, Salikhov TR, Galiakhmetov RN, Shabunina OV, Kopchuk DS, Kovalev IS, Mustafin AG. Nanofibrous carbon (multi-wall carbon nanotubes): synthesis and electrochemical studies by using field-effect transistor setup. Chimica Techno Acta. 2024;11(4):202411421. doi:10.15826/chimtech.2024.11.4.21
12. Nguyen VH, Papanastasiou DT, Resende J, Bardet L, Sannicolo T, Jiménez C, Muñoz-Rojas D, Nguyen ND, Bellet D. Advances in flexible metallic transparent electrodes. Small. 2022;18(19):2106006. doi:10.1002/smll.202106006
13. Ma Y, Zhi L. Graphene-based transparent conductive films: material systems, preparation and applications. Small Methods. 2019;3(1):1800199. doi:10.1002/smtd.201800199
14. Truong KT, Pham TH, Tran KV. The impact of dimethylformamide on the synthesis of graphene quantum dots derived from graphene oxide. Chimica Techno Acta. 2023;10(4). doi:10.15826/chimtech.2023.10.4.05
15. Putri YE, Wendari TP, Arham RA, Muharmi M, Satria D, Rahmayeni R, Wellia DV. Optical response of SrTiO$_3$ thin films grown via a sol-gel-hydrothermal method. Chimica Techno Acta. 2023;10(1):202310108. doi:10.15826/chimtech.2023.10.1.08
16. Liu Y, Xie J, Liu L, Fan K, Zhang Z, Chen S, Chen S. Inkjet-printed highly conductive poly (3, 4-ethylenedioxythiophene): poly (styrenesulfonate) electrode for organic light-emitting diodes. Micromachines. 2021;12(8):889. doi:10.3390/mi12080889
17. Jang W, Kim BG, Seo S, Shawky A, Kim MS, Kim K, Mikladal B, Kauppinen EI, Maruyama S, Jeon I, Wang DH. Strong dark current suppression in flexible organic photodetectors by carbon nanotube transparent electrodes. Nano Today. 2021;37:101081. doi:10.1016/j.nantod.2021.101081
18. Feng X, Wang L, Huang YYS, Luo Y, Ba J, Shi HH, Pei Y, Zhang S, Zhang Z, Jia X, Lu B. Cost-effective fabrication of uniformly aligned silver nanowire microgrid-based transparent electrodes with higher than 99% transmittance. ACS Appl Mater Interfaces. 2022;14(34):39199-39210. doi:10.1021/acsami.2c09672
19. Lancellotti L, Bobeico E, Della Noce M, Mercaldo LV, Usatii I, Veneri PD, Bianco GV, Sacchetti A, Bruno G. Graphene as non conventional transparent conductive electrode in silicon heterojunction solar cells. Appl Surf Sci. 2020;525:146443. doi:10.1016/j.apsusc.2020.146443
20. Jantzen T, Hack K, Yazhenskikh E, Müller M. Thermodynamic assessment of oxide system In$_2$O$_3$-SnO$_2$-ZnO. Chimica Techno Acta. 2018;5(4):166–88. doi:10.15826/chimtech.2018.5.4.02
21. Hofmann AI, Cloutet E, Hadziioannou G. Materials for transparent electrodes: from metal oxides to organic alternatives. Adv Electron Mater. 2018;4(10):1700412. doi:10.1002/aelm.201700412
22. Sharma DK, Shukla S, Sharma KK, Kumar V. A review on ZnO: Fundamental properties and applications. Mater Today: Proc. 2022;49:3028–35. doi:10.1016/j.matpr.2020.10.238
23. Egorova AV, Belova KG, Animitsa IE, Morkhova YA, Kabanov AA. Effect of zinc doping on electrical properties of LaAlO$_3$ perovskite. Chimica Techno Acta. 2021;8(1):20218103. doi:10.15826/chimtech.2020.8.1.03
24. Grivel JC. Subsolidus phase equilibria of the CuO–SrO–ZnO pseudoternary system in air at 900 °C. Chimica Techno Acta. 2018;5(1):6–15. doi:10.15826/chimtech.2018.5.1.01

25. Maraeva E, Radaykin D, Bobkov A, Permiakov N, Matveev V, Maximov A, Moshnikov V. Sorption analysis of composites based on zinc oxide for catalysis and medical materials science. Chimica Techno Acta. 2022;9(4). doi:10.15826/chimtech.2022.9.4.22

26. Ponja SD, Sathasivam S, Parkin IP, Carmalt CJ. Highly conductive and transparent gallium doped zinc oxide thin films via chemical vapor deposition. Sci Rep. 2020;10(1):638. doi:10.1038/s41598-020-57532-7

27. Özgür Ü, Avrutin V, Morkoç H. Zinc oxide materials and devices grown by molecular beam Epitaxy. In Molecular Beam Epitaxy. 2018:343–75. doi:10.1016/B978-0-12-812136-8.00016-5

28. Berumen-Torres JA, Quiñones-Galvan JG, Durán-Muñoz H, Guzmán CH, Torres-Delgado G, Ortega-Sigala JJ, Araiza-Ibarra JJ, Castanedo-Pérez R. Low resistivity annealed tin-doped zinc oxide thin films prepared by the sol gel technique. Mater Sci Eng: B. 2021;268:115134. doi:10.1016/j.mseb.2021.115134

29. Ejsmont A, Goscianska J. Hydrothermal synthesis of ZnO superstructures with controlled morphology via temperature and pH optimization. Mater. 2023;16(4):1641. doi:10.3390/ma16041641

30. Abdel-Galil A, Hussien MS, Yahia IS. Synthesis and optical analysis of nanostructured F-doped ZnO thin films by spray pyrolysis: Transparent electrode for photocatalytic applications. Opt Mater. 2021;114:110894. doi:10.1016/j.optmat.2021.110894

31. Choi D. The transmittance modulation of ZnO/Ag/ZnO flexible transparent electrodes fabricated by magnetron sputtering. J Nanosci Nanotechnol. 2020;20(1):379–83. doi:10.1166/jnn.2020.17238

32. Parihar V, Raja M, Paulose R. A brief review of structural, electrical and electrochemical properties of zinc oxide nanoparticles. Rev Adv Mater Sci. 2018;53(2):119–30. doi:10.1515/rams-2018-0009

33. Matei E, Busuioc C, Evanghelidis A, Zgura I, Enculescu M, Beregoi M, Enculescu I. Hierarchical functionalization of electrospun fibers by electrodeposition of zinc oxide nanostructures. Appl Surf Sci. 2018;458:555–63. doi:10.1016/j.apsusc.2018.06.143

34. Maraeva EV, Permiakov NV, Kedruk YY, Gritsenko LV, Abdullin KA. Creating a virtual device for processing the results of sorption measurements in the study of zinc oxide nanorods. Chimica Techno Acta. 2020;7(4):154–58. doi:10.15826/chimtech.2020.7.4.03

35. Noman MT, Amor N, Petru M. Synthesis and applications of ZnO nanostructures (ZONSs): A review. Crit Rev Solid State Mater Sci. 2022;47(2):99–141. doi:10.1080/10408436.2021.1886041

36. Adedokun O. Review on Transparent Conductive Oxides Thin Films deposited by Sol-gel spin coating technique. Int J Eng Sci Appl. 2018;2(3):88–97.

37. Chen Z, Wang J, Wu H, Yang J, Wang Y, Zhang J, Bao Q, Wang M, Ma Z, Tress W, Tang Z. A transparent electrode based on solution-processed ZnO for organic optoelectronic devices. Nat Commun. 2022;13(1):4387. doi:10.1038/s41467-022-32010-y

38. Zhang D, Yu W, Zhang L, Hao X. Progress in the synthesis and application of transparent conducting film of AZO (ZnO: Al). Mater. 2023;16(16):5537. doi:10.3390/ma16165537

39. Mia MNH, Habiba U, Pervez MF, Kabir H, Nur S, Hossen MF, Sen SK, Hossain MK, Iftekhar MA, Rahman MM. Investigation of aluminum doping on structural and optical characteristics of sol–gel assisted spin-coated nano-structured zinc oxide thin films. Appl Phys A. 2020;126:1–12. doi:10.1007/s00339-020-3332-z

40. Balaprakash V, Gowrisankar P, Sudha S, Rajkumar R. Aluminum doped ZnO transparent conducting thin films prepared by sol-gel dip coating technique for solar cells and optoelectronic applications. Mater Technol. 2018;33(6):414–20. doi:10.1080/10667857.2018.1455384

41. Murugesan M, Arjunraj D, Mayandi J, Venkatachalapathy V, Pearce JM. Properties of Al-doped zinc oxide and In-doped zinc oxide bilayer transparent conducting oxides for solar cell applications. Mater Lett. 2018;222:50–3. doi:10.1016/j.matlet.2018.03.097

42. Istrate AI, Nastase F, Mihalache I, Comanescu F, Gavrila R, Tutunaru O, Romanitan C, Tucureanu V, Nedelcu M, Müller R. Synthesis and characterization of Ca doped ZnO thin films by sol–gel method. J Sol-Gel Sci Technol. 2019;92:585–97. doi:10.1007/s10971-019-05144-7

43. Che L, Song J, Yang J, Chen X, Li J, Zhang N, Yang S, Wang Y. Fluorine, chlorine, and gallium co-doped zinc oxide transparent conductive films fabricated using the sol-gel spin method. J Materiomics. 2023;9(4):745–53. doi:10.1016/j.jmat.2023.02.002

44. Ko D, Gu B, Cheon J, Roh JS, Kim CS, Jo S, Hyun DC, Kim J. Decoupling the contributions to the enhancement of electrical conductivity in transparent silver nanowire/zinc oxide composite electrodes. Mater Chem Phys. 2019;223:634–40. doi:10.1016/j.matchemphys.2018.11.053

45. Aghazadehchors S, Nguyen VH, Munoz-Rojas D, Jiménez C, Rapenne L, Nguyen ND, Bellet D. Versatility of bilayer metal oxide coatings on silver nanowire networks for enhanced stability with minimal transparency loss. Nanoscale. 2019;11(42):19969–79. doi:10.1039/C9NR05658K

46. Tigan D, Genlik SP, Imer B, Unalan HE. Core/shell copper nanowire networks for transparent thin film heaters. Nanotechnol. 2019;30(32):325202. doi:10.1088/1361-6528/ab19c6

47. Nizameev IR, Muscat AJ, Motyakin MV, Grishin MV, Zakharova LYa, Nizameeva GR, Kadirov MK. Surfactant templated oriented 1-D nanoscale platinum and palladium systems on a modified silicon surface. Nano-Structures Nano-Objects. 2019;17:1–6. doi:10.1016/j.nanoso.2018.10.004

48. Nizameev I, Nizameeva G, Kadirov M. Transparent Conductive Layer Based on Oriented Platinum Networks. ChemistrySelect. 2019;4:13564–68. doi:10.1002/slct.201904293

49. Balasubramani V, Chandraleka S, Rao TS, Sasikumar R, Kuppusamy MR, Sridhar TM. Recent advances in electrochemical impedance spectroscopy based toxic gas sensors using semiconducting metal oxides. J Electrochem Soc. 2020;167,:037572. doi:10.1149/1945-7111/ab77a0

50. Balasubramani V, Sureshkumar S, Rao TS, Sridhar TM. Impedance spectroscopy-based reduced graphene oxide-incorporated ZnO composite sensor for H_2S investigations. ACS omega. 2019;4:9976–9982. doi:10.1021/acsomega.9b00754

51. Nizameev IR, Nizameeva GR, Faizullin RR, Kadirov MK. Oriented nickel nanonetworks and its submicron fibres as a basis for a transparent electrically conductive coating. ChemPhysChem. 2021;22:288–92. doi:10.1002/cphc.202000876

52. Nizameev IR, Nizameeva GR, Kadirov MK. Doping of Transparent Electrode Based on Oriented Networks of Nickel in Poly (3, 4-Ethylenedioxythiophene) Polystyrene Sulfonate Matrix with P-Toluenesulfonic Acid. Nanomaterials. 2023;13(5):831. doi:10.3390/nano13050831

53. Nizameeva GR, Gainullin RR, Lebedeva EM, Nizameev IR. Gas Sensing Element of a Conductometric Nitrogen Dioxide Sensor Based on Oriented Nickel Oxide Networks. High Energ Chem. 2023;57(Suppl 1):S45–S49. doi:10.1134/S0018143923070299

54. Swanepoel R. Determination of the thickness and optical constants of amorphous silicon. J Phys E Sci Instrum. 2000;16(12):1214–22. doi:10.1088/0022-3735/16/12/023

55. Sanchez-Gonzalez J, Dıaz-Parralejo A, Ortiz AL, Guiberteau F. Determination of optical properties in nanostructured thin films using the Swanepoel method. Appl Surf Sci. 2006;252(17):6013–17. doi:10.1016/j.apsusc.2005.11.009

56. Kumar S, Kumar A, Kumar A, Krishnan V. Nanoscale zinc oxide-based heterojunctions as visible light active photocatalysts for hydrogen energy and environmental remediation. Catalysis Rev. 2020;62(3):346–405. doi:10.1080/01614940.2019.1684649

57. Udayachandran Thampy US, Mahesh A, Sibi KS, Jawahar IN, Biju V. Enhanced photocatalytic activity of ZnO–NiO nanocomposites synthesized through a facile sonochemical route. SN Appl Sci. 2019;1:1–15. doi:10.1007/s42452-019-1426-z

58. Hashim M, Usman M, Ahmad S, Shah R, Ali A, Rahman NU. ZnO/NiO nanocomposite with enhanced photocatalytic H2 production. Int J Photoenergy. 2024;(1): 2676368. doi:10.1155/2024/2676368

59. Chen Z, Li W, Li R, Zhang Y, Xu G, Cheng H. Fabrication of highly transparent and conductive indium–tin oxide thin films with a high figure of merit via solution processing. Langmuir. 2013;29(45):13836–13842. doi:10.1021/la4033282

60. Jiang S, Hou PX, Chen ML, Wang BW, Sun DM, Tang DM, Jin Q, Guo QX, Zhang DD, Du JH, Tai KP, Tan J, Kauppinen EI, Liu C, Cheng HM. Ultrahigh-performance transparent conductive films of carbon-welded isolated single-wall carbon nanotubes. Sci Adv. 2018;4(5):eaap9264. doi:10.1126/sciadv.aap92

61. Kang J, Han K, Sun X, Zhang L, Huang R, Ismail I, Wang Z, Ding C, Zha W, Li F, Luo Q, Li Y, Lin J, Ma CQ. Suppression of Ag migration by low-temperature sol-gel zinc oxide in the Ag nanowires transparent electrode-based flexible perovskite solar cells. Org Electron. 2020;82:105714. doi:10.1016/j.orgel.2020.105714